

A method is presented to maintain one-dimensional heat transport in variably saturated soil cells over freezing and thawing temperatures. It applies transient thermal boundary conditions and replicates field-scale ground thaw. The method allows the isolated study of coupled heat and transport in permafrost environments.

A.A. Mohammed, Dep. of Earth Sciences, Univ. of Western Ontario, 1151 Richmond Street N, London, ON, N6A 5B7 Canada, currently at Dep. of Geoscience, Univ. of Calgary, 2500 University Drive NW, Calgary, AB, T2N 1N4 Canada; R.A. Schincariol, Dep. of Earth Sciences, Univ. of Western Ontario, 1151 Richmond Street N, London, ON, N6A 5B7 Canada; R.M. Nagare, Water Business Unit, Worley Parsons Canada, 4445 Calgary Trail, Edmonton, AB, T6H 5R7 Canada; and W.L. Quinton, Cold Regions Research Centre, Wilfrid Laurier Univ., 75 Avenue West, Waterloo, ON, N2L 3C5 Canada. *Corresponding author (amohamme@ucalgary.ca).

Vadose Zone J.
doi:10.2136/vzj2014.01.0008
Received 15 Jan. 2014.

© Soil Science Society of America
5585 Guilford Rd., Madison, WI 53711 USA.

All rights reserved. No part of this periodical may be reproduced or transmitted in any form or by any means, electronic or mechanical, including photocopying, recording, or any information storage and retrieval system, without permission in writing from the publisher.

Reproducing Field-Scale Active Layer Thaw in the Laboratory

Aaron A. Mohammed,* Robert A. Schincariol, Ranjeet M. Nagare, and William L. Quinton

A method to simulate freeze–thaw and permafrost conditions on a large peat–soil column, housed in a biome, was developed. The design limits ambient temperature interference and maintains one-dimensional freezing and thawing. An air circulation system, in a cavity surrounding the active layer, allows manipulation of the lateral temperature boundary by actively maintaining an air temperature matching the average temperature of the soil column. Replicating realistic thermal boundary conditions enabled field-scale rates of active-layer thaw. Radial temperature gradients were small and temperature profiles mimicked those for similar field conditions. The design allows complete control of key hydrologic processes related to heat and water movement in permafrost terrains without scaling requirement; and presents a path forward for the large-scale experimental study of frozen ground processes. Because subarctic ecosystems are very vulnerable to climate and anthropogenic disturbances, the ability to simulate perturbations to natural systems in the laboratory is particularly important.

Abbreviations: ATI, ambient temperature interference.

Permafrost and active-layer processes occur over approximately 25% of the Earth's surface (Williams and Smith, 1989) and play a vital role in the hydrologic functioning of northern watersheds (Woo and Winter, 1993). Layered peat deposits underlain by permafrost are geographically extensive and pervade large areas of arctic, subarctic, and boreal environments (Woo and Winter, 1993). High-latitude warming trends and increased anthropogenic activities stress the need for a comprehensive understanding of the mechanisms responsible for permafrost sustainability in these sensitive ecosystems. Because peat hydraulic conductivity generally decreases by several orders of magnitude with depth (Quinton et al., 2000), active-layer thicknesses strongly influence the drainage characteristics of these northern landscapes (Wright et al., 2009). For example, Zhang et al. (2010) concluded, in a study of infiltration into peat-covered permafrost soils, that the single most important factor controlling infiltration is ground thaw depth. Active-layer thickness is controlled by heat and water transfer between the ground surface and the underlying permafrost table (Hayashi et al., 2007). The freezing and thawing of soils induces both water and heat movement (Harlan, 1973). These processes are not independent as water flows under matric and thermal gradients, while moving water transports energy and affects soil thermal properties (Hoekstra, 1966). In variably saturated media, because frozen soil retains water, freezing temperatures perturb the soil pressure–saturation equilibrium, resulting in steep gradients that redistribute water from warmer to colder zones (Dirksen and Miller, 1966). As a result of this tight coupling and nonlinear nature, problems related to water and heat transport are often difficult to study in the field and can benefit from controlled laboratory work where the important climatic and physical properties can be isolated and investigated (Zhou et al., 2006).

The primary mechanism controlling ground heat flux through the shallow subsurface to the frost table is often heat conduction (Hayashi et al., 2007). In a natural terrestrial environment, any arbitrary soil column will be radially insulated by the soil around it, so temperature forcing is primarily downward from ground surface temperatures. This means

that thermal gradients and heat conduction are effectively vertical and one-dimensional (Hayashi et al., 2007). Creating an experimental setup that can simulate one-dimensional vertical heat flow is critical to being able to adequately replicate field conditions. For example, both Zhou et al. (2006) and Nagare et al. (2012a) stressed the importance of minimizing ambient temperature interference (ATI) in their coupled heat and water movement laboratory studies. This interference creates lateral temperature gradients that make maintaining one-dimensional thermal gradients challenging (Prunty and Horton, 1994). This often results in studies using sample volumes that may be too small to capture field-scale processes and limits the use of field instrumentation within the sample. Work done by others to reduce ATI have used passive insulation methods, the most effective of which was presented by Zhou et al. (2006) and utilized by Gieselman et al. (2008) and Heitman et al. (2007) for experiments with and without freezing conditions, respectively. These studies used insulated soil cells with a concentric layer of the same soil at similar moisture conditions. This method is very effective for experiments of relatively short duration (e.g., 46 d for Gieselman et al., 2008) but fails for longer periods of time because no insulation can be perfect. Ambient temperature interference will eventually cause lateral temperature gradients; this is especially true for conditions where very steep lateral thermal gradients between the sample and its surroundings exist. Thus, passive insulation may not be suitable for experiments where ATI needs to be minimized for a longer time period than can be achieved with passive methods. For studies investigating the field-scale hydrologic implications of freezing and thawing, larger samples that allow the establishment of realistic thermal and moisture gradients for longer periods of time (i.e., many months) are required. Such experiments therefore require careful instrumentation and alternative approaches to reduce ATI and validate field-scale conditions (Henry, 2007; Lewis and Sjöström, 2010).

We have developed an experimental method that reduces radial temperature gradients at a scale, and under boundary conditions, that replicate coupled heat and water movement in permafrost environments. We made use of the two-level climate chamber presented by Nagare et al. (2012b) designed for large-scale study of active layer–permafrost systems. The experiment described by Nagare et al. (2012a) and a subsequent study by Nagare et al. (2012b) highlight the effect of freezing on the active-layer hydrology of permafrost peatlands. Our experiment used a new soil column designed to maintain one-dimensional thermal gradients under longer term, field-rate freezing and thawing conditions. The previous experimental setup was able to sustain one-dimensional thermal gradients only under less demanding freezing conditions for shorter periods of time. It is easier to maintain one-dimensional thermal gradients in the laboratory during freezing conditions because of the permafrost boundary condition; freezing occurs from both ends. This means that the soil column reaches the freezing point relatively quickly, due to two freezing fronts, and the entire active layer remains under the zero-degree curtain for a long

period of time (Carey and Woo, 2005). Once the active layer is completely frozen, there is less temperature variation in the vertical direction in the soil profile as it changes gradually with depth. Thawing, however, occurs only from the top down, and this creates a stark temperature difference between the thawing front and the soil profile above it (Quinton and Hayashi, 2008). Establishing realistic ground thaw conditions in a controlled environment can give insight into parameters controlling the thermal regime of the active layer during thawing.

The goal of the design was to limit ATI by placing the soil column concentrically within another larger container and radially insulating the soil by circulating air within the cavity between the two containers. Our hypothesis was that while the column was exposed to transient temperature boundary conditions at its ends, we could actively manipulate the temperature within the cavity to reflect the average temperature in the active-layer portion of the soil column and reduce lateral thermal gradients. The air space and the outer volume of soil were expected to buffer the 30-cm-diameter core, where the instrumentation is housed. This setup enables ATI to be minimized while the soil column is exposed to a range of transient temperatures associated with freezing and thawing. We provide data highlighting the column's ability to maintain one-dimensional freezing and thawing front movement.

Materials and Methods

Climate Chamber

The climate chamber used was that presented by Nagare et al. (2012a), a unique two-level biome capable of simulating large-scale subsurface environments (Fig. 1). The chamber consists of an upper and lower level, allowing soil monoliths to be placed between the two levels separated by an adjustable insulated floor, as shown in Fig. 2. Both levels of the chamber are capable of simulating a temperature range from 40 to -40°C . Additional climatic controls in the upper level include light intensity, relative humidity, rain, and CO_2 concentrations. Situating part of a monolith in the lower chamber allows the simulation of the permafrost condition common to subarctic peatlands: a saturated base layer that remains frozen while the rest of the column in the upper level can be exposed to a variety of climatic conditions. This proxy permafrost is crucial to simulating the upward redistribution of water during freezing, which is not possible with the combination of cold plates and heat exchangers used in other studies (Nagare et al., 2012a). A full description of the climate chamber and its capabilities were provided by Nagare et al. (2012a).

Experimental Setup

Temperature and soil conditions simulated in this experiment were based on field studies conducted at Scotty Creek, NWT, Canada. Scotty Creek is a 152-km^2 basin located in the lower Liard River valley in the central part of the Mackenzie River basin, and is

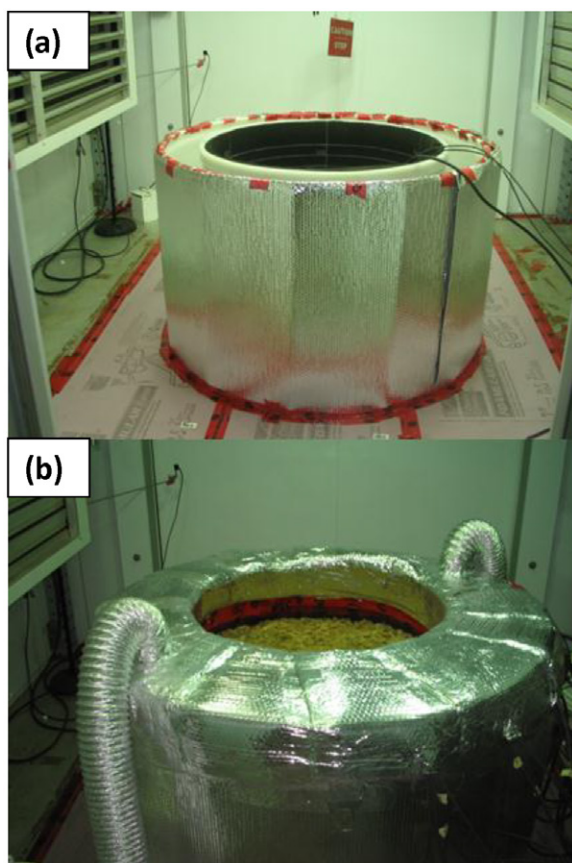


Fig. 1. (a) Two-column design to create air-filled cavity, and (b) final instrumented soil column.

characteristic of wetland-dominated basins found within the zone of discontinuous permafrost (Wright et al., 2008). This region is located close to the southern limit of the discontinuous permafrost zone and represents one of the permafrost ecosystems most vulnerable to climate warming and human disturbances (Quinton and Baltzer, 2012).

Temperature settings in the upper and lower levels of the climate chamber provide the vertical boundary conditions of the soil monolith, i.e., permafrost and ground surface temperatures. To ensure one-dimensional heat transport and the reduction of lateral thermal gradients, a number of new design measures were undertaken.

The monolith setup consists of two low-density polyethylene cylindrical containers (U.S. Plastic Corp.), one placed inside the other. The inner and outer containers have internal diameters of approximately 90 and 120 cm, respectively, and both are 120 cm in depth. The inner container houses the soil and instrumentation as described below. Placing it in the second container creates an air space isolating the sides of the soil column from the conditions in the upper level of the climate chamber. This creates a cavity where air can be circulated to reduce the lateral gradients imposed by the temperature setting of the upper chamber. The temperature of the air space can then be adjusted manually to reflect the

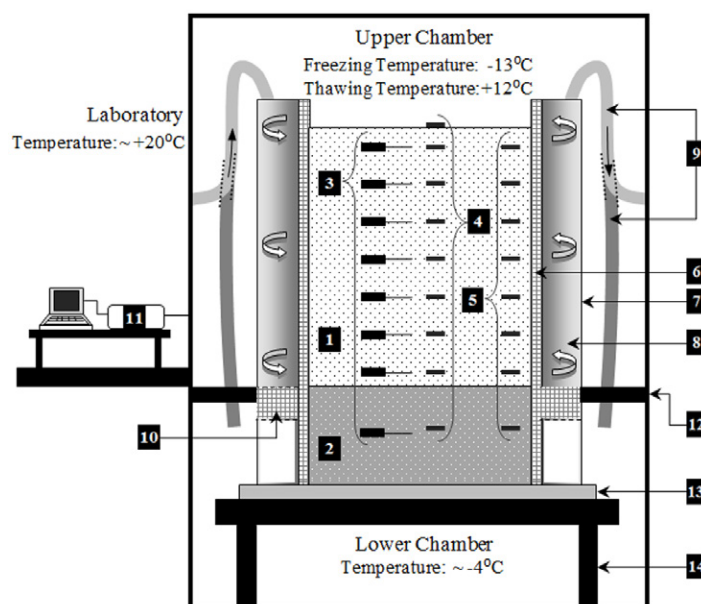


Fig. 2. Experimental setup (not drawn to scale): (1) 65-cm-deep active layer, (2) 40-cm bottom frozen layer, (3) time domain reflectometry probes, (4) thermistor probes (center), (5) thermistor probes (edge), (6) inner low-density polyethylene (LDPE) container lined with neoprene foam, (7) outer LDPE container insulated with Reflectix from outside, (8) cavity in which air is circulated, (9) ducting through which air is circulated into and out of the cavity, (10) 15-cm-thick Neoprene band separating airspace from lower chamber, (11) multiplexers and datalogger connected to a personal computer, (12) adjustable insulated floor separating upper and lower chambers, (13) weighing scale, and (14) frame to support monolith.

average temperature of the active layer. What this effectively does is dampen the temperature to which the sides of soil column are exposed, while giving the ability to actively manipulate temperatures in the cavity as the thermal regime of the active layer changes during freezing and thawing.

Seasonal fluctuations in air and ground surface temperatures decrease in amplitude with depth because of the thermal buffering capacity of soil. This creates a time lag in response to changes in surface temperature and results in active-layer temperatures that are warmer than the surface in winter and cooler in summer. For laboratory simulations, this means that during freezing, warmer air is needed to warm the cavity, and during thawing, cooler air is needed to cool it. Figure 2 illustrates how this was achieved. The air space was sealed off from the upper chamber environment with the exception of two 10-cm (4-inch) diameter ports where insulated aluminum ducting was attached to provide an inlet and outlet for air to be circulated within the cavity. The system makes use of the differences in ambient temperatures of the upper chamber, lower chamber, and room temperature of the laboratory in which the chamber is located. Air that is warmer or cooler (depending on whether freezing or thawing) is vented into the cavity through the inlet, with the outlet maintaining circulation. The two ducting configurations are shown in Fig. 2 and illustrate the port differences for freezing and thawing cycles. When the active layer is

undergoing freezing, laboratory air that is at approximately 20°C is circulated in the cavity. This incoming air is cooled by the ambient temperature of the upper chamber (−13°C), creating a blended air temperature that can be manipulated to match the average temperature of the active layer. During thawing, when cooler air is needed in the cavity, air is vented from the lower chamber (−4°C) such that the blended temperature reflects the thermal regime of the active layer. For both configurations, the outlet vents back to the inlet source of air.

To control the airflow and temperature within the cavity, a muffin fan (24 V DC, Sanyo Denki) was attached in-line to the inlet ducting. The fan was connected to a proportional controller with an integral temperature control (System 350 A350P, Johnson Controls). A temperature sensor was placed within the cavity and attached to the controller. The integral temperature control regulates the fan speed based on the temperature to which the controller is set. The fan speed is automatically adjusted to achieve the desired temperature in the cavity. The air in the cavity is isolated from the upper chamber in terms of air flow; however, the temperature within the cavity will be affected by the temperature in the upper chamber. This is not a major issue because the air circulation rate will adjust to maintain the desired temperature.

In addition to the temperature-controlled air circulated through the cavity, the inner container was lined with 2.54-cm-thick closed-cell neoprene foam. This provided additional insulation and ensured a tight seal between the peat and container (Nagare et al., 2012a). The outer container was insulated with two layers of reflective bubble wrap (Reflectix). The portion of the cavity that is situated in the lower chamber was partitioned from that in the upper chamber by a 15-cm-thick layer of neoprene foam. This ensures that the air is circulated only within the active layer of the soil column, keeping the soil in the lower chamber frozen and under a stable temperature regime.

Soil Column Packing and Instrumentation

The soil column was constructed using repacked peat in an effort to simulate a natural peatland profile characteristic of those found in the zone of discontinuous permafrost, while allowing us to reduce the effect of small-scale heterogeneities such as macropores and rooting zones. Although these small-scale heterogeneities can affect thaw development by processes such as infiltration (Kane et al., 2001), they are not representative of the thermal properties of the bulk soil matrix, which is what controls thaw at the basin scale due to conduction (Hayashi et al., 2007). Peatlands exhibit a layered stratigraphy due to the

degradation and consolidation of the organic matter that comprises the soil type. As such, the transition from fibric to well-decomposed humic peat translates to a depthwise change in its physical and hydraulic properties (Quinton et al., 2000).

The base of the soil column consisted of a 40-cm layer packed with unprocessed humified peat to a bulk density of 250 kg m^{−3}. Once packed, this layer was saturated and allowed to freeze to represent the ice-rich saturated permafrost. A 65-cm active layer was packed above this using sphagnum moss matching the density profile at Scotty Creek as documented by Hayashi et al. (2007) (see Fig. 3a and 3b). Although the base of the soil column was frozen before packing the active layer, the top of the frozen layer was exposed at the surface to above-freezing temperatures during packing of the active layer. When packing, therefore, the interface between the permafrost and the active layer was thawed (approximate 5 cm thick) to provide continuity between layers and for better placement of sensors at this interface.

Time-domain reflectometry (TDR) probes (CS10 with SDMX multiplexers connected to a TDR100, Campbell Scientific) were used to measure the unfrozen water content. Additional instrumentation included temperature sensors (107BAM with an absolute accuracy of 0.2–0.5°C, multiplexed using an AM16/32B, Campbell Scientific) placed in the center and edge of all instrumented depths (see Fig. 2). Calibration of the TDR probes utilized Maxwell–De

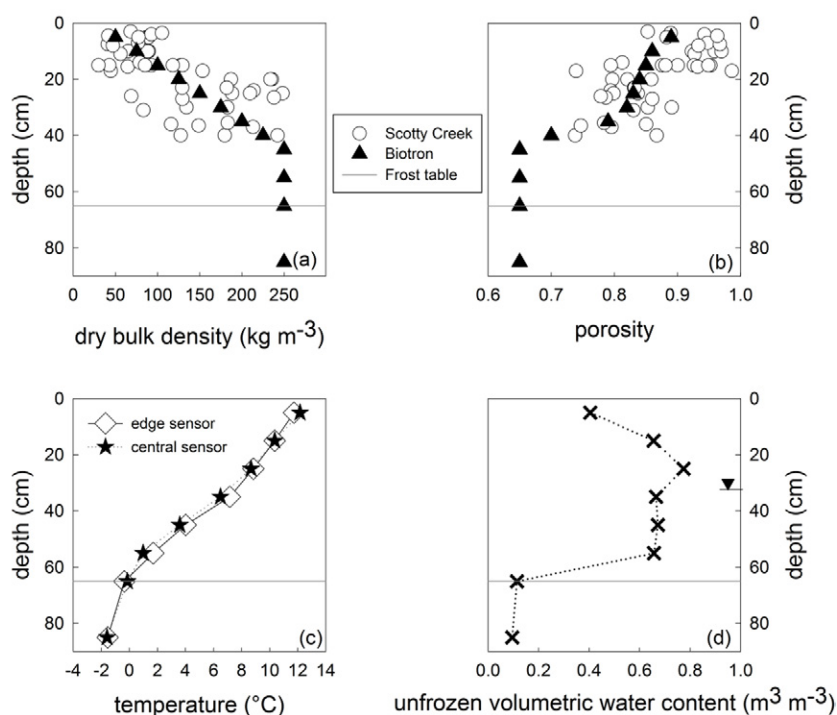


Fig. 3. Biotron soil column and Scotty Creek field site (a) density and (b) porosity profiles (Scotty Creek data obtained from Hayashi et al. [2007], deeper peat density values in soil column based on Zhang et al. [2008]) and soil column (c) initial temperature and (d) water content profiles; water table depth is indicated by the inverted triangle symbol at 35 cm. Frost table depths on all plots are for the Biotron experiment.

Loor's four-phase mixing model, details of which can be found in Nagare et al. (2011). Porosity values at different depths used in the mixing model were determined using small samples of the same peat used in the monolith, packed to the same bulk densities. All instrumentation was connected to dataloggers (CR1000, Campbell Scientific), and values were measured and recorded every 15 min.

Experimental Conditions

Upper and lower temperatures were initially held at 20 and -4°C , respectively, to establish stable temperature and water content profiles. At the onset of the freezing cycle, the water table was approximately 35 cm below the soil surface. Upper-level temperature (a proxy for air temperature) was then sequentially dropped to -13°C during a period of 36 d to simulate winter conditions; -13°C is the average winter ground surface temperature at Scotty Creek (Wright et al., 2009). Once the column was completely frozen and the temperature profile stable, the upper-level temperature was sequentially increased from -13 to 12°C (the average ground surface temperature at Scotty Creek when air temperatures are consistently above 0°C), allowing 45 cm of the active layer to undergo thawing. Initial liquid water content and temperature distributions are shown in Fig. 3c and 3d.

Results

Radial Temperature Differences and Temperature Distribution

A key objective of the experiment was to replicate freeze–thaw processes at a scale that would allow the realistic representation of coupled heat and water transport in permafrost environments. Thus the degree to which one-dimensional freezing and thawing front propagation was maintained has to be taken in context with the accuracy of typical field sensors also used in the experiment. While studies on smaller soil cells, such as that of Zhou et al. (2006), achieved better minimization of radial temperature gradients, such techniques are not applicable at the scales simulated in this study.

Lateral temperature gradients, measured by radial differences between thermistors in the center and at the edge of the monolith, were used as one way to examine the influence of ATI. The temperature time series in Fig. 4 shows that the design, as expected, was better able to maintain one-dimensional conditions during the freezing cycle than the thawing cycle. Temperature distributions within the column throughout the experiment,

illustrated in Fig. 5, also highlight the setup's ability to maintain one-dimensional temperature profiles. Differences in the shapes of the temperature profiles on Days 0 and 330 were probably due to more time being needed to establish steady-state conditions under the 20°C upper boundary. This is because the upper chamber temperature was only increased from 12 to 20°C toward the end of the thawing cycle to ensure that the 45-cm depth thawed (Fig. 4).

Figures 4 and 5 show that the greatest radial temperature differences are evident in the uppermost measurement depth (5 cm), with thaw differences of $\leq 3.0^{\circ}\text{C}$. The differences diminish with

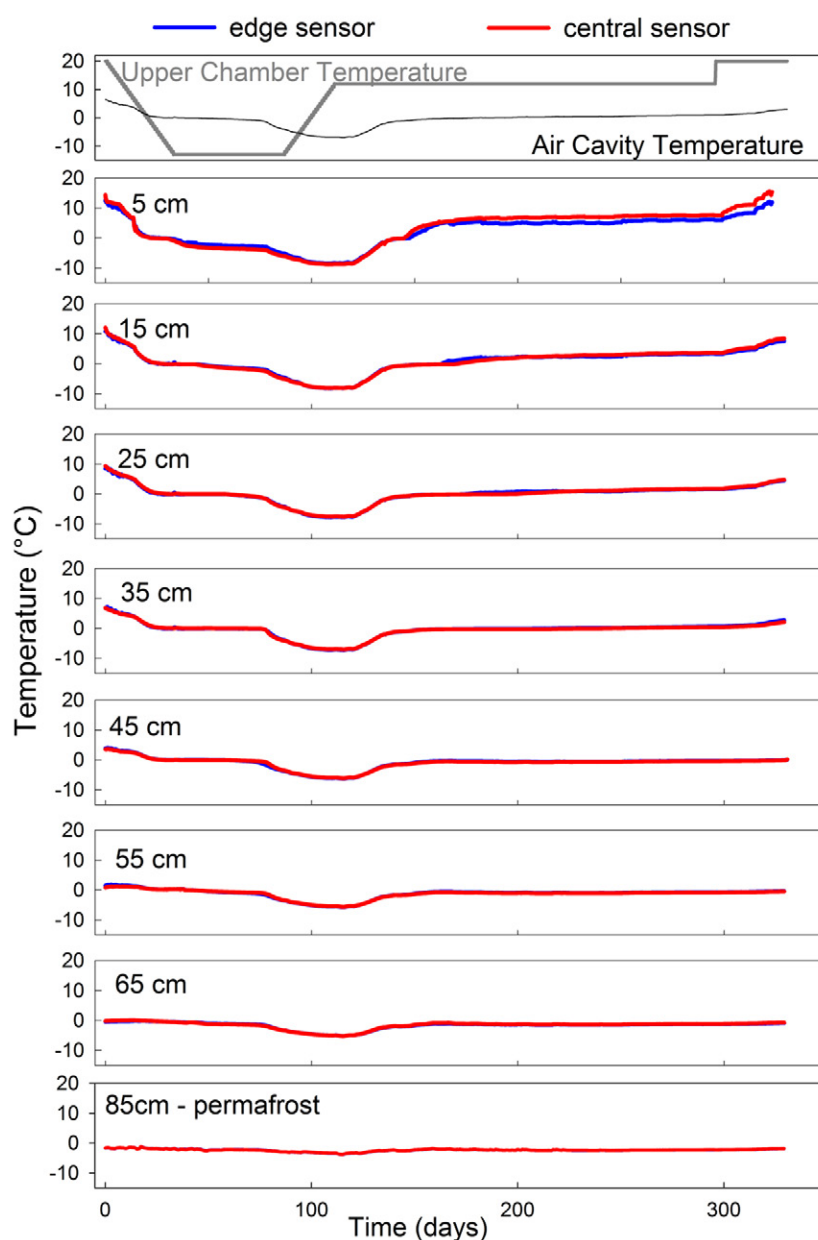


Fig. 4. Temperature time series for all instrumented depths (5–85 cm) in the soil column, as well as the upper chamber and air cavity temperatures in the upper panel. Data from the central and edge sensors nearly completely overlap each other and thus the edge sensor cannot be seen for 45 cm and deeper.

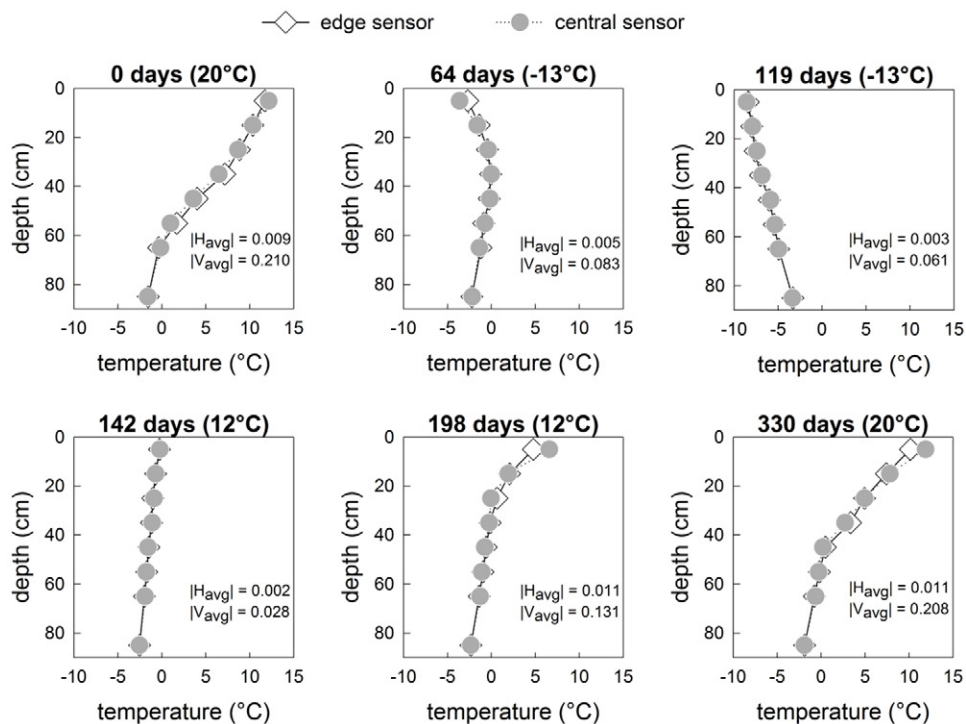


Fig. 5. Temperature distribution profiles at different time periods for center and edge thermistors. Upper chamber temperature settings are shown in parentheses next to each time period. On the right of each graph are the calculated values of average horizontal ($|H_{avg}|$) and vertical ($|V_{avg}|$) gradients (in $^{\circ}\text{C cm}^{-1}$) for the 65-cm active layer.

depth to $\leq 1.0^{\circ}\text{C}$; results below 5 cm are comparable to the work of others (Zhou et al., 2006; Heitman et al., 2007).

The difficulty in maintaining one-dimensional thermal conditions during thaw arises from the permafrost boundary condition. Freezing occurs from both ends, which means that the soil column reaches the freezing temperature relatively quickly and the entire active layer remains under the zero-degree curtain for a significant period of time. As can be seen in Fig. 5, this makes minimizing lateral temperature gradients easier because the cavity air temperature (providing the radial temperature boundary) is more representative of the soil temperatures. However, thawing occurs only from the top down; during thaw, the phase changes (and thus zero-degree curtain effect) with depth occur during a longer period of time. The result is that the thaw front propagates downward more slowly than when the same distance is covered by two bidirectional freezing fronts. This creates a large temperature contrast between the thawing front and the thawed soil profile above it, such that soil temperatures within the column cover a wider range than during freezing. For example, as shown in Fig. 5, at Day 119, freezing temperatures in the soil profile ranged from approximately -3 to -9°C , while during thawing at Day 330, temperatures ranged from approximately -2.5 to 14°C . The observation that temperature gradients are largest during thaw is well supported by field studies such as those of Carey and Woo (2001) and Quinton and Hayashi (2008). Freezing and thawing front progression is also slower in

peat than in mineral soils because latent heat effects become more dominant within peat soils, which have high volumetric water contents. Thus the portion of the soil column most affected by ATI was the uppermost 5 cm, which had the highest porosity (Fig. 3b). Peat exhibits much higher porosities than most soils, suggesting that results with this design should be even better for mineral soils.

Freezing and Thawing Curves

During periods of phase change, ground heat flux is dominated by latent energy exchange to freeze or thaw the active layer (Roulet and Woo, 1986). During thawing, a small amount of energy may go to warm the active layer and permafrost because of the unfrozen water present in frozen soils (Farouki, 1981). During periods of phase change, the temperature remains under the zero-degree curtain at discrete depths within the active layer until the end of the phase change. In

the field during thawing, this period of phase change extends from the time the ground becomes free of snow in the spring until late summer when the frost table reaches the bottom of the active layer. The relationship between liquid water content and temperature during this process is illustrated by soil freezing and thawing characteristic curves (Fig. 6). If heat transport is assumed to be vertically unidimensional, then one of the fundamental requirements when generating freeze–thaw curves is that measurements of temperature and unfrozen moisture content in a time series are made at the same depth and lie on the same spatial plane (perpendicular to heat flow).

Significant lateral temperature gradients, and thus non-one-dimensional freezing and thawing front movement across the core's 30-cm diameter can be interpreted from the freezing and thawing curves in Fig. 6. Lateral freezing and thawing is evident as a deviation of the curve from vertical during the zero-degree curtain period, indicating a temperature increase or decrease from the freezing point before all phase change has occurred and the liquid moisture content has stabilized. This deviation is clearly present in the uppermost 5-cm layer of the soil column during the late periods of thawing; it can be seen that before the maximum liquid water content (approximately 0.3) was reached, temperatures began to rise, indicating that energy was being partitioned to sensible heat. This significantly diminished in deeper layers, shown by the other freezing and thawing curves almost completely overlapping

each other during freezing and thawing periods. However, deviations in the surface layers are expected not to be important because under field conditions snowmelt infiltration results in advective heat transfer and thus non-uniform freeze–thaw processes. The decrease in moisture on thaw completion in the 5- to 25-cm depth was due to evaporation at positive temperatures.

A good illustration of the freeze–thaw curves in the relative absence of other processes is the 35-cm-depth curves, where both before and after phase change, moisture content is relatively stable. Overall, the freeze–thaw curves compare well with those reported for the field, as reported by Quinton and Hayashi (2008) and also shown in Fig. 6. The Scotty Creek curves exhibit some hysteresis between freezing and thawing cycles. This is illustrated as the thawing curve deviating slightly from the general freezing temperature toward the end of phase change. This slight hysteresis may be attributed to (i) non-vertical heat movement and the effect of lateral heat transfer, as was evident in the 5-cm depth of this study, or (ii) differences in pore-scale interfacial tension–temperature relations for different pore sizes depending on whether undergoing freezing or thawing (Smerdon and Mendoza, 2010). The latter will be expected to be more evident in peat with higher porosity and thus shallower depths; however, the results of this study show that it is not strongly correlated with depth, as porosity certainly is; porosity decreases with depth due to increased consolidation (Fig. 3a and 3b). Our results indicate that in the absence of lateral heat transfer, hysteresis is tremendously diminished. This is very interesting to note because recently there have been divergent theories on the cause of thermal hysteresis in freezing soils from field and laboratory data (Smerdon and Mendoza, 2010; Parkin et al., 2013; Kurylyk and Watanabe, 2013). This may mean that it is other heat transfer effects, not taken into account in conceptual models, rather than the osmotic and matric potential differences proposed by some researchers (e.g., Smerdon and Mendoza, 2010). One possible alternative explanation is that the hysteresis is linked to differences in antecedent water storage: any upward moisture redistribution during freezing may increase water content during thawing compared with freezing. Water is a heat-carrying mass, thus larger relative amounts of water at the time of thawing may enhance sensible heat effects and cause the slight deviation from the zero-degree curtain during the latter period of soil thawing (see Scotty Creek curves in Fig. 6).

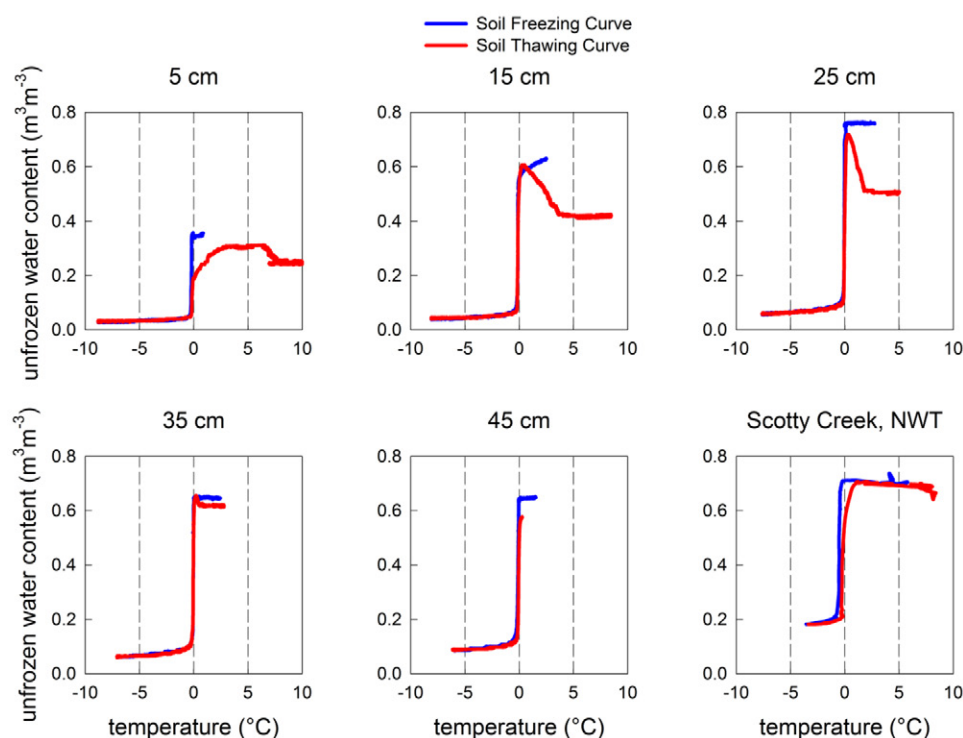


Fig. 6. Soil freezing and thawing curves for the 5- to 45-cm depth of the laboratory soil column and the 30-cm depth of an instrumented soil pit at Scotty Creek from the 2002–2003 field season (Scotty Creek data obtained from Quinton and Hayashi, 2008).

Thermal Regime and Thaw Time

A very important simulation parameter is the length of time taken to thaw the active layer. The thaw time in this study was approximately 200 d, which compares relatively well with the 156-d thawing period observed at the field site by Wright (2009). Also, a comparison of the thermal regimes in the soil column and at Scotty Creek clearly shows the experiment's ability to reproduce the full range of temperature distributions observed in the field (Fig. 7).

Thawing was halted at a depth of 45 cm (Fig. 7) to begin preparing the column for a subsequent freezing cycle. The possible reasons for a longer thaw time than observed in the field are: (i) the experiment did not simulate the effect of precipitation and snowpack and thus lacked an external source of water (and its associated energy), and (ii) the thawing temperature was held at 12°C, which represents the average thawing-period temperature at Scotty Creek and not the higher temperatures experienced in late summer, which is when maximum thaw depths are reached (Wright et al., 2009). While simulating precipitation and a snowpack is possible in the climate chamber, the purpose of this study was to simply validate the design and its ability to simulate one-dimensional heat transport. The infiltration of snowmelt water affects the thaw process because the thermal conductivity of the soil increases with increasing moisture content; the thermal conductivity of water is approximately 22 times that of air (Hillel, 1998). In addition, the absence of a snowpack in this study resulted in evaporation beginning earlier in the thawing

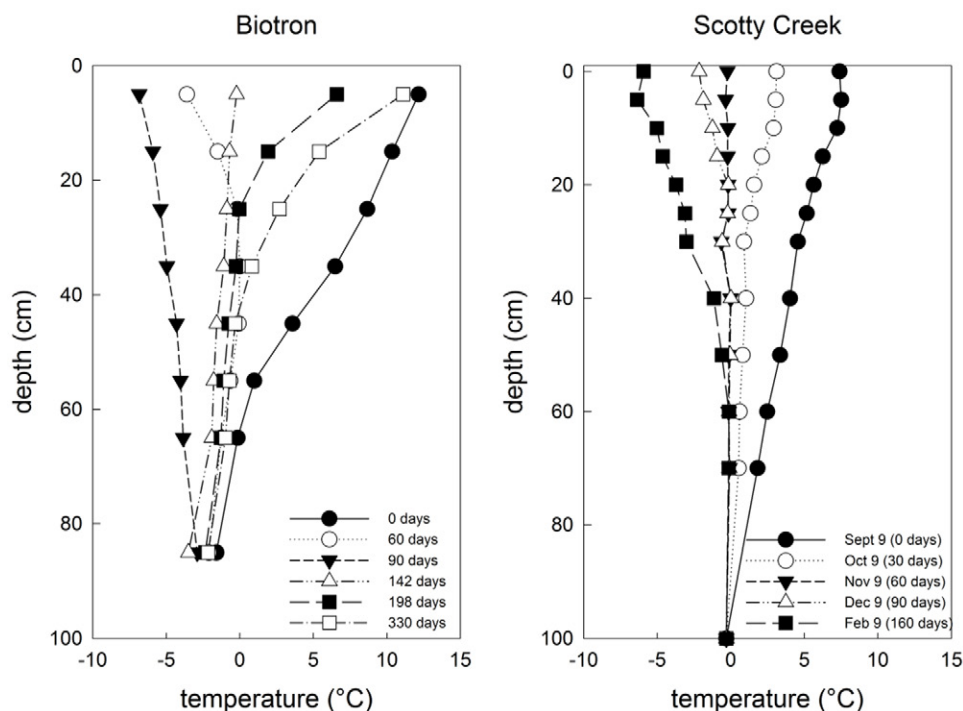


Fig. 7. Thermal regime during entire freeze-thaw cycle for the soil column experiment and Scotty Creek field site (November 2001–February 2002). The temperature at the 100-cm depth for Scotty Creek was approximated from the Norman Wells pipeline (Smith et al., 2004).

period than it would in the field. Decreases in moisture content and energy from the active layer due to evaporation decreases the rate of heat conduction and slows thaw-front progression. Because the temperature was maintained at 12°C, combined with the decreased thermal conductivity from evaporative water loss, thawing toward the latter end of the run slowed and started to approach steady state as the thermal regime stabilized under the temperature boundary conditions. This stabilization required that the temperature in the upper chamber be increased to 20°C toward the end of the thawing cycle for the 45-cm depth to completely thaw, as can be seen in Fig. 4.

Discussion and Conclusions

This study was able to simulate field-scale heat and water transfer in a soil column through an experiment that reduced lateral thermal gradients, while a unique two-level biome maintained permafrost and surface temperatures at the vertical ends of a soil column. The active-layer portion of the monolith consists of an inner peat column insulated by an air-filled cavity. Temperature-controlled air is circulated within the cavity that represents the average temperature of the active layer and acts as a buffer from the ambient temperature of the climate chamber. Results show that the experimental design was successful in minimizing lateral temperature gradients to a reasonable degree of accuracy given the large scale of the soil column. The minimization of these gradients allows the physical simulation of

one-dimensional active-layer thawing, which is what occurs in nature. The thaw rate observed here was validated by field observations.

Other experimental studies aimed at reducing ATI have all used passive methods of insulation (e.g., soil or insulation materials). Because no insulation is perfect, this limits the time scale of experiments and the range of freezing and thawing temperatures to which soil cells can be exposed. An active method, however, like that used here, allows the temperature in the insulation air space to be adjusted to accommodate active-layer freeze-thaw thermal regime changes. This in turn enables the use of a larger range of temperatures that more closely resemble field conditions. Realistic thermal regimes are required to study the impact of climate changes on hydrologic and ecological processes. Although a very sophisticated climate chamber was

used in this study, the methodology used here is transferable to simpler, or more complex, climate chambers and can be down- or upscaled. Thus the described methodology could improve studies using hot and cold plates or heat exchangers (Dirksen and Miller, 1966; Hoekstra, 1966; Fukuda et al., 1980; Stähli and Stadler, 1997) and more complex studies as proposed by French and Olsen (2012). It is simply the application of a transient radial temperature boundary condition.

The methodology proposed and validated here provides a path forward for the large-scale experimental study of coupled heat and water transport on frozen soils. In particular, for the apparatus and climate chamber discussed, the effect of complex surface variables such as vegetation, snowpack, and winter snowmelt events can now be studied. Such laboratory studies, when coupled with field studies to constrain and validate parameters, are critical to understanding the effects of environmental stressors on the hydrologic cycles of sensitive permafrost ecosystems. This is a major issue in cold region studies due to the tight coupling of heat and water movement and the nonlinear feedbacks that control the thermal, hydrologic, and ultimately ecological functioning of these landscapes.

Acknowledgments

We wish to acknowledge the financial support of the Natural Science and Engineering Research Council of Canada (NSERC) and BioChambers Inc. (MB, Canada) through a NSERC-CRD award, NSERC Strategic Projects grant, and the Canadian Space Agency (CSA) through a Capacity Building in SS&T Cluster Pilot grant. We also thank Roger Peters, Steve Bartlett, Jon Jacobs, and Marc Schincariol for their assistance in the laboratory.

References

- Carey, S.K., and M.K. Woo. 2001. Slope run-off processes and flow generation in a subarctic, subalpine environment. *J. Hydrol.* 253:110–129. doi:10.1016/S0022-1694(01)00478-4
- Carey, S.K., and M.K. Woo. 2005. Freezing of subarctic hillslopes, Wolf Creek Basin, Yukon, Canada. *Arct. Antarct. Alp. Res.* 37:1–10. doi:10.1657/1523-0430(2005)037[0001:FOSHCW]2.0.CO;2
- Dirksen, C., and R.D. Miller. 1966. Closed-system freezing of unsaturated soil. *Soil Sci. Soc. Am. Proc.* 30:168–173. doi:10.2136/sssaj1966.03615995003000020010x
- Farouki, M. 1981. The thermal properties of soils in cold regions. *Cold Reg. Sci. Technol.* 3:223–232.
- French, H.K., and O. Olsen. 2012. Bioklima proposal. Bioforsk, Ås, Norway. http://www.bioforsk.no/ikbViewer/Content/99634/20121017_Bioklima%20IIFinal.pdf
- Fukuda, M., A. Orhun, and J.N. Luthin. 1980. Experimental studies of coupled heat and moisture transfer in soils during freezing. *Cold Reg. Sci. Technol.* 5:67–75.
- Gieselman, H., J.L. Heitman, and R. Horton. 2008. Effect of a hydrophobic layer on the upward movement of water under surface freezing conditions. *Soil Sci.* 173:297–305. doi:10.1097/SS.0b013e31816d1e75
- Harlan, R.L. 1973. Analysis of coupled heat–fluid transport in partially frozen soil. *Water Resour. Res.* 9:1314–1323. doi:10.1029/WR009i005p01314
- Hayashi, M., N. Goeller, W.L. Quinton, and N. Wright. 2007. A simple heat conduction method for simulating the frost table depth in hydrological models. *Hydrol. Processes* 21:2610–2622. doi:10.1002/hyp.6792
- Heitman, J.L., R. Horton, T. Ren, and T.E. Ochsner. 2007. An improved approach for measurement of coupled heat and water transfer in soil cells. *Soil Sci. Soc. Am. J.* 71:872–880. doi:10.2136/sssaj2006.0327
- Henry, H.A.L. 2007. Soil freeze–thaw cycle experiments: Trends, methodological weaknesses and suggested improvements. *Soil Biol. Biochem.* 39:977–986. doi:10.1016/j.soilbio.2006.11.017
- Hillel, D. 1998. *Environmental soil physics*. 2nd ed. Academic Press, New York.
- Hoekstra, P. 1966. Moisture movement in soils under temperature gradients with cold-side temperature below freezing. *Water Resour. Res.* 2:241–250. doi:10.1029/WR002i002p00241
- Kane, D.L., K.M. Hinkel, D.J. Goering, L.D. Hinzman, and S.I. Outcalt. 2001. Nonconductive heat transfer associated with frozen soils. *Global Planet. Change* 29:275–292. doi:10.1016/S0921-8181(01)00095-9
- Kurylyk, B.L., and K. Watanabe. 2013. The mathematical representation of freezing and thawing processes in variably-saturated, non-deformable soils. *Adv. Water Resour.* 60:160–177. doi:10.1016/j.advwatres.2013.07.016
- Lewis, J., and J. Sjöström. 2010. Optimizing the experimental design of soil columns in saturated and unsaturated transport experiments. *J. Contam. Hydrol.* 115:1–13. doi:10.1016/j.jconhyd.2010.04.001
- Nagare, R.M., R.A. Schincariol, W.L. Quinton, and M. Hayashi. 2011. Laboratory calibration of time domain reflectometry to determine moisture content in undisturbed peat samples. *Eur. J. Soil Sci.* 62:505–515. doi:10.1111/j.1365-2389.2011.01351.x
- Nagare, R.M., R.A. Schincariol, W.L. Quinton, and M. Hayashi. 2012a. Moving the field into the lab: Simulation of water and heat transport in subarctic peat. *Permafrost Periglacial Processes* 23:237–243.
- Nagare, R.M., R.A. Schincariol, W.L. Quinton, and M. Hayashi. 2012b. Effects of freezing on soil temperature, freezing front propagation and moisture redistribution in peat: Laboratory investigations. *Hydrol. Earth Syst. Sci.* 16:501–515. doi:10.5194/hess-16-501-2012
- Parkin, G., A. von Bertoldi, and A.J. McCoy. 2013. Effect of tillage on soil water content and temperature under freeze–thaw conditions. *Vadose Zone J.* 12(1). doi:10.2136/vzj2012.0075
- Prunty, L., and R. Horton. 1994. Steady-state temperature distribution in nonisothermal, unsaturated closed soil cells. *Soil Sci. Soc. Am. J.* 58:1358–1363. doi:10.2136/sssaj1994.03615995005800050011x
- Quinton, W.L., and J.L. Baltzer. 2012. The active-layer hydrology of a peat plateau with thawing permafrost (Scotty Creek, Canada). *Hydrogeol. J.* 21:201–220. doi:10.1007/s10040-012-0935-2
- Quinton, W.L., D.M. Gray, and P. Marsh. 2000. Subsurface drainage from hummock-covered hillslope in the Arctic tundra. *J. Hydrol.* 237:113–125. doi:10.1016/S0022-1694(00)00304-8
- Quinton, W.L., and M. Hayashi. 2008. Recent advances towards physically-based runoff modeling of the wetland-dominated Central Mackenzie River Basin. In: M. Woo, editor, *Cold Region atmospheric and hydrological studies: The Mackenzie GEWEX Experience*. Vol. 2. Hydrologic processes. Springer-Verlag, Berlin. p. 257–279.
- Roulet, N.T., and M.-K. Woo. 1986. Hydrology of a wetland in the continuous permafrost region. *J. Hydrol.* 89:73–91. doi:10.1016/0022-1694(86)90144-7
- Smerdon, B.D., and C.A. Mendoza. 2010. Hysteretic freezing characteristics of riparian peatlands in the Western Boreal Forest of Canada. *Hydrol. Processes* 24:1027–1038. doi:10.1002/hyp.7544
- Smith S.L., M.M. Burgess, D. Riseborough, T. Coulfish, and J. Chartrand. 2004. Digital summary database of permafrost and thermal conditions: Norman Wells Pipeline study sites. Open File 4635. Geol. Surv. Canada, Ottawa, ON.
- Stähli, M., and D. Stadler. 1997. Measurement of water and solute dynamics in freezing soil columns with time domain reflectometry. *J. Hydrol.* 195:352–369. doi:10.1016/S0022-1694(96)03227-1
- Williams, P.J., and M.W. Smith. 1989. *The frozen earth: The fundamentals of geocryology*. Cambridge Univ. Press, New York.
- Woo, M.K., and T.C. Winter. 1993. The role of permafrost and seasonal frost in the hydrology of wetlands in North America. *J. Hydrol.* 141:5–31. doi:10.1016/0022-1694(93)90043-9
- Wright, N. 2009. Water and energy fluxes from a permafrost peat plateau: Examining the controls on runoff generation. Ph.D. diss. Simon Fraser Univ., Burnaby, BC, Canada.
- Wright, N., M. Hayashi, and W.L. Quinton. 2009. Spatial and temporal variations in active-layer thawing and their implication on runoff generation in peat-covered permafrost terrain. *Water Resour. Res.* 45:W05414. doi:10.1029/2008WR006880
- Wright, N., W.L. Quinton, and M. Hayashi. 2008. Hillslope runoff from an ice-cored peat plateau in a discontinuous permafrost basin, Northwest Territories, Canada. *Hydrol. Processes* 22:2816–2828. doi:10.1002/hyp.7005
- Zhang, Y., S.K. Carey, and W.L. Quinton. 2008. Evaluation of the algorithms and parameterizations for ground thawing and freezing simulation in permafrost regions. *J. Geophys. Res.* 113:D17116. doi:10.1029/2007JD009343
- Zhang, Y., S.K. Carey, W.L. Quinton, J.R. Janowicz, J.W. Pomeroy, and G.N. Flerchinger. 2010. Comparison of algorithms and parameterizations for infiltration into organic-covered permafrost soils. *Hydrol. Earth Syst. Sci.* 14:729–750. doi:10.5194/hess-14-729-2010
- Zhou, J., J.L. Heitman, R. Horton, T. Ren, T.E. Ochsner, L. Prunty, et al. 2006. Method for maintaining one-dimensional temperature gradients in unsaturated closed soil cells. *Soil Sci. Soc. Am. J.* 70:1303–1309. doi:10.2136/sssaj2005.0336N